Role of Landing Energy in E-Beam Metrology of Thin Photoresist for High-NA EUVL

Mohamed Zidan[a,b,*], **Daniel Fischer**[c], **Joren Severi**[a,b], **Danilo De Simone**[b], **Alain Moussa**[b], **Angelika Müllender**[c], **Chris Mack**[d], **Anne-Laure Charley**[b], **Philippe Leray**[b], **Stefan De Gendt**[a,b], **Gian Francesco Lorusso**[b]
[a]KU Leuven, Celestijnenlaan 200F, 3001 Leuven, Belgium
[b]imec, Kapeldreef 75, 3001 Leuven, Belgium
[c]Carl Zeiss SMT GmbH, Carl-Zeiss-Straße 22, 73447 Oberkochen, Germany
[d]Fractilia, Austin Texas, USA

Abstract.
Background: Lithography advancements require resist layer thickness reduction, essential to cope with the low depth of focus (DOF) characteristic of high numerical aperture extreme ultraviolet lithography (HNA EUVL). However, such a requirement poses serious challenges in terms of resist process metrology and characterization, as patterns in thin resist suffer from low contrast, which may affect the performance of the edge detection algorithms used for image analysis, ultimately impacting metrology.
Aim: Investigate e-beam imaging using low landing energy (LE) settings as a possible way to address the thin resist film metrology issues.
Approach: A low-voltage aberration-corrected SEM developed at Carl Zeiss is to image three thin resist thicknesses and two different underlayers, at various LE and number of frames. All images are analyzed using MetroLER software, to extract the parameters of interest [mean critical dimension (CD), line width roughness (LWR), and linescan signal-to noise-ratio (SNR)] in a consistent way.
Results: The results indicate that mean CD and LWR are affected by the measurement conditions, as expected. Imaging through landing energy unravels two opposing regimes in the mean CD estimate, the first in which the mean CD increases due to charging and the second in which the mean CD decreases due to shrinkage. Additionally, the trend between LE and linescan SNR varies depending on the stack.
Conclusion: We demonstrated the ability of low-voltage aberration-corrected SEM to perform thin resist metrology with good flexibility and acceptable performance. The landing energy proved to be an important knob for metrology of thin resist.

Keywords: thin resist, HNA EUVL, BKM, e-beam, LVSEM, landing energy, high resolution.

*Mohamed Zidan, Email: Mohamed.Zidan@imec.be

1 Introduction

The transition towards high numerical aperture extreme ultraviolet lithography (HNA EUVL) is the natural progression of the semiconductor roadmap to enable future technology nodes (N2 and beyond) and to pattern sub-10 nm features. Resist film thickness has to scale to cope with the depth of focus (DOF), as per the second Rayleigh equation, which decreases by the square of the numerical aperture.[1] Additionally, a pattern aspect ratio of 2:1 between the height and width is required to prevent pattern collapse. Advanced technology nodes in high-NA EUV environment are expected to require resist thickness in the range 10-20 nm for line and space features (LS). These thicknesses may pose serious challenges in terms of resist metrology and characterization, affecting the Signal-to-Noise ratio (SNR) in critical dimension scanning electron microscopy (CDSEM) as well as in other metrology tools, ultimately impacting precision, roughness, and CD measurements.[2]

A possible way to address these challenges consists in using a primary electron beam at lower landing energies (LE). Lower landing energies are attractive for imaging the thin resist because of the smaller interaction volume between the electrons and the sample, hence higher lateral surface sensitivity. Additionally, the imaging contrast can be controlled by changing the landing energy.[3] In general, in the case of thinner resist, the pattern is expected to have a better contrast at such lower landing energies, where the interaction volume is smaller, as illustrated in figure 1 (A) for a situation where the underlayer is not charged. The trend will depend however on the materials used in the stack.

The resist line and the underlayer space regions are directly irradiated by the e-beam during measurements. The resists and underlayers have distinct chemical composition, therefore their secondary electron emission yields are different. Considering the typical secondary (or total) electron emission yield curves of the material, the yield becomes larger than 1 when lowering the landing energy. In this regime, the number of secondary electrons emitted from the resist line is larger than the number of primary electrons penetrating the sample, so that the surface will become positively charged.[3–5] However, although charging of the resist and the underlayer is expected when shifting towards the low landing energy regime, the charging artifacts will have different magnitudes, as they depend on the different material yield curves for resist and underlayer. Moreover, the trajectory of the emitted electrons from the resist line edge might be influenced by charging in the underlayer as shown in figure 1 (B). This effect will introduce additional artifacts related to the specific materials stack being used.

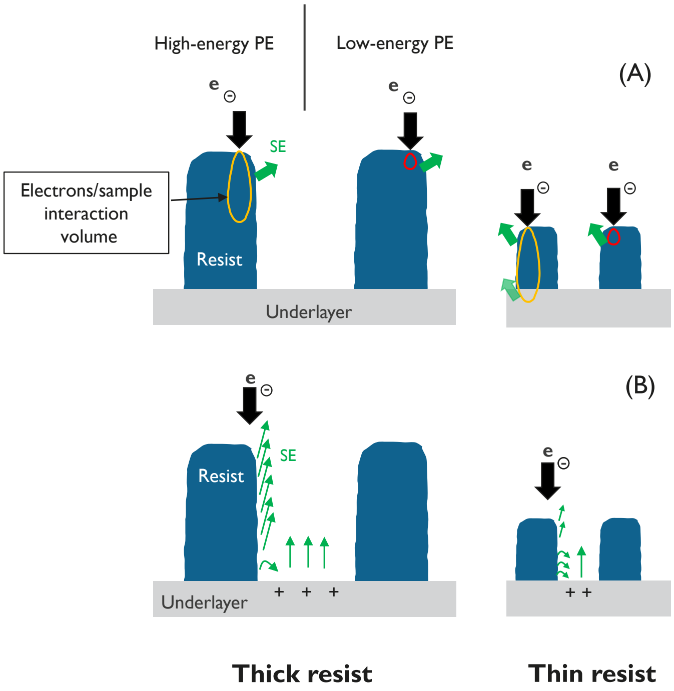

Fig 1 (A) Interaction volume for high and low landing energy on thick and thin resist. (B) Effect of a charged underlayer on the emitted secondary electrons for thick and thin resist.

Even though imaging with low energy e-beam has its advantages, it is technically challenging to build a microscope capable of meeting the tight requirement in this regime. In fact, chromatic aberrations and the energy spread may lead to reduction in resolution, increasing the beam diameter, and deteriorating imaging contrast. Moreover, the electron wavelength is inversely proportional to its energy, so that low energy electrons have larger wavelengths, causing electron diffraction and reduced depth of field.[6] Furthermore, additional challenges appear in the electron-optical system when shifting towards low beam energies, because of the degraded performance of emitters at such energies. In state-of-the-art instruments, these issues are addressed by designing the columns specifically to decelerate electrons to lower energies (either at the sample stage or in the column) while the electron source emits at constant operating energies.[7] The SEM apparatus used in this study is specifically designed to achieve low landing energies and to reduce diffraction and aberrations in order to maintain high resolution in the low landing energies regime, as it will be explained in the next section.

In this paper, we investigate in detail the influence of using low landing energy and varying integration frame number on thin resist metrology for EUVL. Mean CD, shrinkage, linescan SNR, line width roughness are investigated for thin film thicknesses (30, 20, and 15 nm) and underlayer type [spin-on glass (SOG) and organic underlayer (UL)].

2 Experiment

2.1 Wafer Stack and Materials

In this study a positive tone, chemically amplified EUV resist at three resist thicknesses (nominally coated at 30, 20, and 15 nm) is used. The resist is patterned on two underlayers, either a siloxane-based spin-on glass (SOG) or a carbon-based organic underlayer (O-UL). The experiment included four conditions, three resist thicknesses at 30, 20, 15 nm on SOG underlayer, plus one condition at 15 nm resist thickness on O-UL. All wafers were patterned with an ASML full-field NXE: 3400 scanner, with 1:1 line and space (LS) pattern at 32 nm pitch. Atomic force microscope (AFM) measurements for the final resist array height after patterning were performed, resulting in 11.8 nm for the 15 nm nominal resist on SOG, 16.1 nm for the 20 nm nominal resist on SOG, 19.6 nm for 30 nm nominal resist on SOG, and 11.4 nm for 15 nm nominal resist on O-UL.

Table 1 Summary of the wafer stack thicknesses, underlayers type and SEM measurement conditions in this experiment.

Resist thickness (nominal) (nm)	Resist thickness (AFM) (nm)	Underlayer type	SEM landing energy (eV)	SEM number of frames
30	19.6	SOG	500, 300, 200, 150	24, 18, 12, 9, 6
20	16.1	SOG	500, 300, 200, 150	24, 18, 12, 9, 6
15	11.8	SOG	500, 300, 200, 150	24, 18, 12, 9, 6
15	11.4	O-UL	500, 300, 200, 150	24, 18, 12, 9, 6

2.2 Low Voltage SEM Apparatus Description

In a typical e-beam microscope operating at ultra-low landing energies regimes, the electron diffraction effects as well as the spherical and chromatic aberrations impose limits on the minimum achievable resolution. The SEM apparatus used in this study is an aberration-corrected SEM developed at Carl Zeiss.[8] The electron column of this microscope is specifically designed to reduce dispersion, astigmatism, aberrations, and image distortion to maintain high lateral resolution (0.6 nm) even at such ultra-low landing energy regime.

The column is equipped with an electron mirror and a beam separator, in addition to the electron gun and condenser lenses, as illustrated in figure 2. Within the whole column, the average kinetic energy of electrons is fixed to a constant value. To achieve a particular low landing energy at the sample, electrons are decelerated only at the end of the objective lens.

The primary electron beam is generated by the thermal field emission gun and focused with the condenser lenses on the beam separator. The three electrostatic condenser lenses adjust the probe current by changing the illuminated area of the aperture and control the magnification at a constant intermediate image plane. The electron beam passes through the beam separator into the mirror section, where the beam is being decelerated towards the mirror plane. At the mirror plane, predefined negative chromatic and spherical aberrations are applied. After reflection at the mirror, the beam is accelerated towards the beam separator again and guided to the objective lens. While passing the objective lens, the beam is decelerated to its final landing energy and the positive lens aberrations are cancelled out by previously infixed negative aberrations.

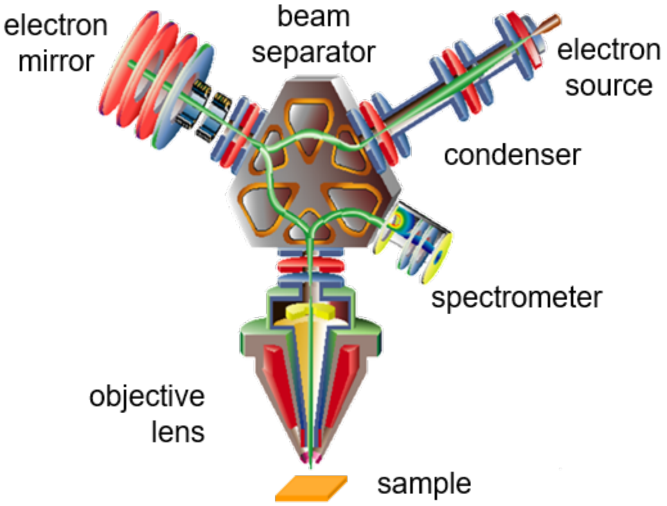

Fig 2 Schematic view of the mirror-corrected scanning electron microscope used in the study.[8]

2.3 *SEM Measurement Conditions and Analysis*

A pixel size of 0.6 nm is used for all the measurements in this experiment. Four landing energies are considered: 500, 300, 200, and 150 eV. The second metrology knob we used is the number of frames of integration, in order to study the effect of frame averaging on the measurements. Averaging of 6, 9, 12, 18, and 24 frames for all landing energies is studied. Other SEM measurements parameters are fixed, specifically, a probe current of 15 pA, a number of pixels in the field of view (FOV) of 2048x1536, and a pixel dwell time of 100 ns are used. For each condition, 30 different positions on the wafer are measured to provide sufficient data for the roughness unbiasing.[9] Each measurement has been statically repeated 5 times at the same position, in order to estimate CD shrinkage and measurement precision. Mean CD, linescan signal-to-noise ratio, and unbiased roughness were estimated by analyzing the images using Fractilia MetroLER software.

3 Results and Discussion

3.1 Low Voltage SEM Image Visibility and Quality Metric for the Thin Resist

A visual comparison of the low voltage scanning electron microscope (LVSEM) images for the 30 and 15 nm thick resist on SOG and O-UL is shown in figure 3. Images are taken at the listed landing energies using 24 frames of integration. It is observed that the image contrast depends on the resist film thickness and the underlayer. The thin resist has less contrast, and the images change with the landing energies, as expected.

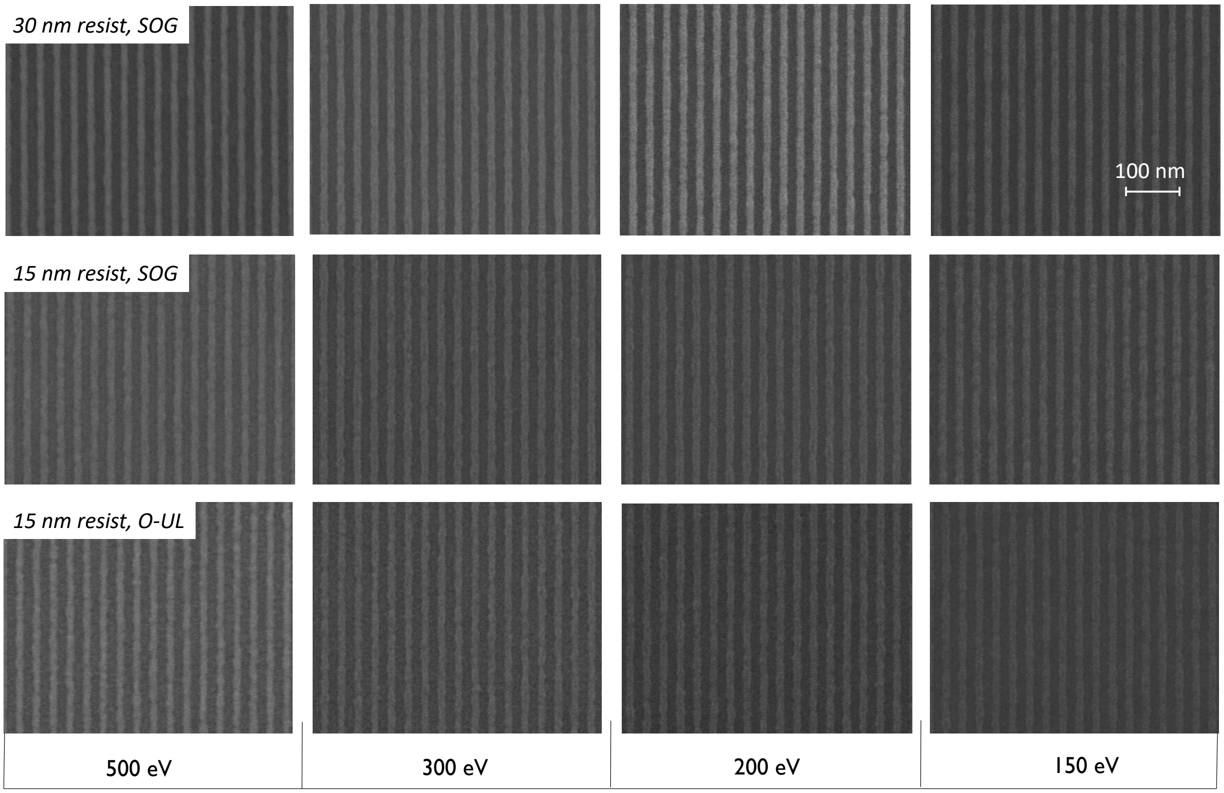

Fig 3 SEM images for the 30 and 15 nm resist with the SOG and O-UL captured at different landing energies and 24 frames.

3.1.1 SNR with the Different SEM Conditions

The signal-to-noise ratio (SNR) measured by MetroLER is used to quantify the CDSEM image quality in different conditions. The SNR is defined as the signal (difference between the minimum and maximum grayscale value for the feature average linescan) divided by the grayscale image noise (1σ). It is calculated for each individual feature, then averaged over the total number of features within the images.

Figure 4 illustrates the effect of reducing the film thickness on the SNR at the different landing energies, as well as the impact of changing the number of frames. Thinner resist layers have lower SNR for all the SEM conditions. In addition, an enhancement of the SNR with the number of frames is observed. This is expected because of the decrease of the grayscale image noise from 6 frames to 24 frames. Finally, the landing energy affects the resulted SNR, however, it's difficult to identify a clear trend.

Both resist and underlayer type are expected to affect the imaging. The influence of the underlayer becomes pronounced when varying the landing energy, because of the different secondary electron emission yield curves between the materials. In addition, when using thin resist, the interaction volume at higher landing energies extends beyond the resist thickness itself, to the underlayer material underneath the resist, thus leading to additional electrons emissions. For example, at 500 eV the penetration depth in resist is about 20 nm.[10]

Figure 5 depicts the linescan SNR trend with the landing energies for the two underlayers types (SOG and O-UL) at the same resist thickness (15 nm). In the case of the SOG, there is a slight dependence of the linescan SNR on the landing energy. On the contrary, the linescan SNR increases with the landing energy for the O-UL. Additionally, at low landing energies (150 and

200 eV), the wafer with SOG underlayer has better linescan SNR compared to the O-UL wafer. At higher landing energies (300 and 500 eV), the O-UL has better SNR compared to the SOG. In order to understand the possible cause of this, the two components of the linescan SNR (the signal and the grayscale noise parts) should be considered separately.

Figure 6 plots the grayscale image noise and difference between the minimum and maximum of the resist linescan intensities for each wafer with the two variations of the underlayer at the different landing energies and number of frames. The first observation is that the grayscale image noise increases with higher landing energies which might indicate the effect of larger extended electrons emission from the underlayers underneath the resist lines because of the larger interaction volume at these energies. Another factor is the dependence of the direct emission of the space region (underlayer) on the landing energy. Secondly, there is small difference between the grayscale image noise values comparing the two underlayers' at landing energies of 200 to 500 eV. At 150 eV landing energy, the O-UL wafer has lesser noise compared to the SOG wafer. Considering the signal part, the difference between the maximum and minimum of the grayscale value of the linescan stack with O-UL shows the increase with shifting to higher landing energies, on the other hand, there is slight change in the signal part with the landing energy in the SOG stack. This difference between the signal part from the two stacks might be accounted for by additional charging effects of the organic underlayer in the space region that eventually impact the secondary electrons emitted from the resist line edges. This illustrates the influence of the stack underlayer on the average linescans of the resist line and image grayscale noise, and points out the metrology challenges with the thin resist when only an underlayer change in the patterning stack can lead to the different metrology conclusions.

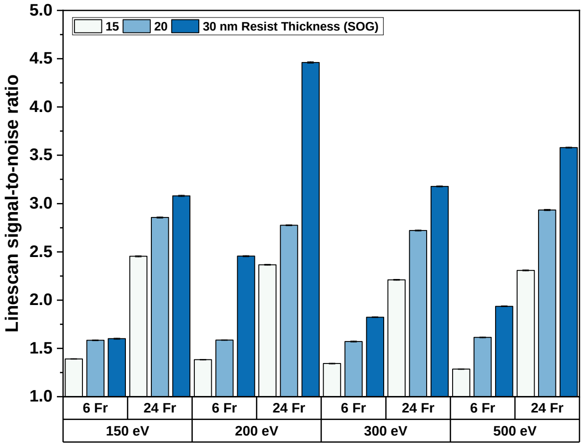

Fig 4 The effect of reducing the resist thickness on the linescan SNR at the different landing energies and number of frames of integration. Thinner resists always show reduced linescan SNR compared to thicker resists at the same measurement conditions.

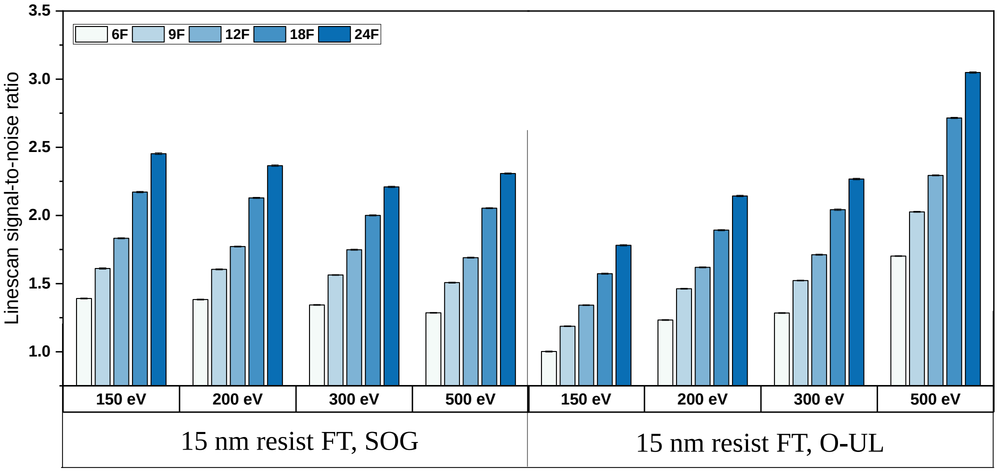

Fig 5 The linescan SNR ratio dependence on the underlayer (O-UL & SOG) at the same resist thickness of 15 nm. Depending on the underlayers, different trends are observed between the SNR and the LE.

Finally, we would like to note that, for each landing energy working point, all images are taken with automatic brightness and contrast adjustment of the photomultiplier tubes (electrical offset and amplification), the PMTs were set to optimal histogram spread with respect to brightness and contrast. This can add uncertainty in the values of the signal and noise reported in this section through the LE. However, this is the standard setup for acquiring the images in any SEM tool.

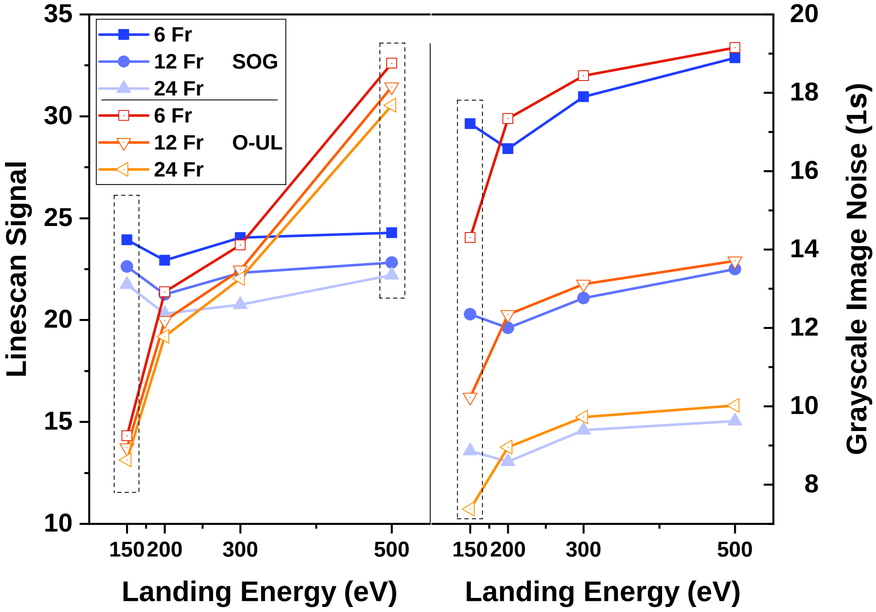

Fig 6 The linescan signal and grayscale image noise plotted separately for the different landing energies and number of frames for the two stacks of SOG and O-UL for the 15 nm resist. The landing energy clearly affects the linescan signal for the O-UL. The error bars on the data are contained in the size of the symbol.

3.2 CD Measurement with the Different SEM Conditions

The feature width extracted from the CDSEM changes with the different measurement conditions. The measured critical dimension value depends on the complex e-beam and materials interactions, surface charging accumulation, physical slimming of the line, and carbon contamination artifacts combined. In the present work, the landing energy and number of frames of integration are the measurement conditions under investigation for the thin resist. The landing energy impacts the interaction volume, penetration depth, and additionally the surface charging. The number of frames controls the electron dose irradiated to the sample which causes the resist feature slimming and image noise level modulation.

The mean CD is plotted for the available landing energies at the different number of frames for the 15 nm resist on SOG, as shown in figure 7. The mean CD is observed to vary with the number of frames at a fixed landing energy or with the landing energy at a fixed number of frames. More specifically, at lower landing energies (150 eV and 200 eV) the mean CD increases when increasing the number of frames. On the contrary, at the higher landing energies (300 eV and 500 eV), there is decrease in the mean CD when using more frames.

At low LE, this magnification effect can be attributed to the phenomenon of positive surface charging of the resist line. The resist is a non-conductive organic material that accumulates charges. At low LE, because the electron interaction is shallow, when using more number of frames, the surface becomes more positively charged. More positively charged line gives an apparent larger CD. At higher LE (300 eV and 500 eV), the interaction volume is deeper, and in this regime positive surface charging is less. The decrease in the mean CD when using more frames can be attributed to resist physical shrinkage by increasing the electron dose.

Surface charging and resist physical shrinkage artifacts are present simultaneously during the measurement, however, which artifact effect becomes dominant will depend on the different SEM conditions. These results have shown that there are two regimes depending on the LE in which either the positive surface charging or shrinkage effects dominate the mean CD measurement. In the low landing energy regime, increasing the number of frames biases the mean CD to larger values, and in the high landing energy regime, increasing the number of frames shrinks the line to smaller CD. Between these two regimes there is a flipping point that separates these two regimes. At this flipping point, the mean CD becomes least dependent on the number of frames used, so it is thought of as a balance point between the artifacts of charging and shrinkage biasing the mean CD estimate.

These trends are consistent for the three resist thicknesses and the two underlayers variations investigated in this study as illustrated in figure 8. The variation in the mean CD values from wafer to wafer is expected due to the difference in the resist thickness and underlayers, however, the trends between the mean CD and SEM conditions, the observation of the two regimes (charging and shrinkage), the presence of the flipping point are found in all wafers.

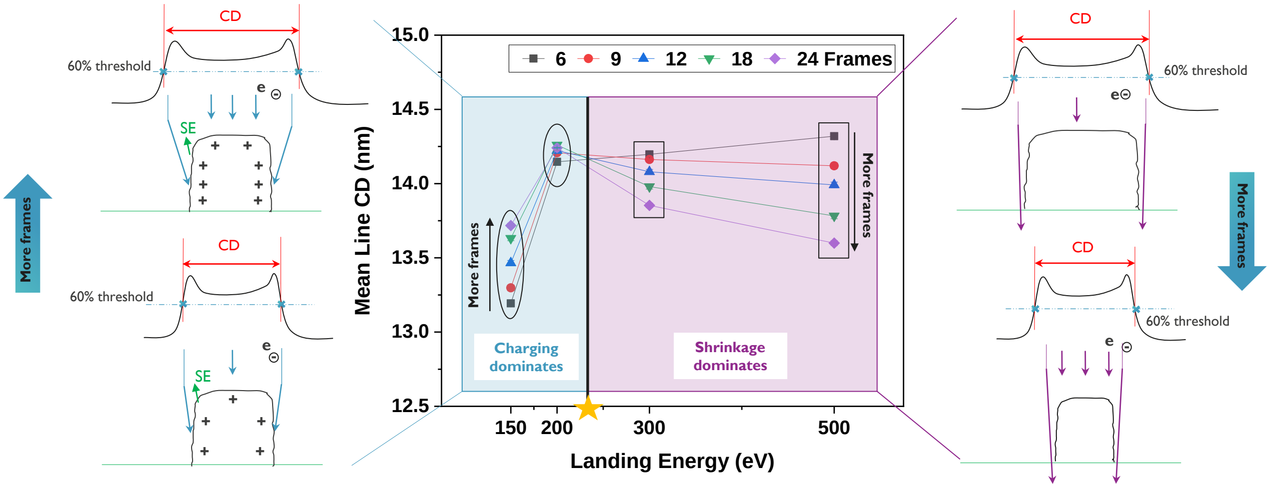

Fig 7 The mean line CD for the 15 nm resist on SOG extracted from SEM images with different landing energies and number of frames. Depending on the LE, the CD estimate is dominated by either charging or shrinkage. Two regimes are separated by a flipping point.

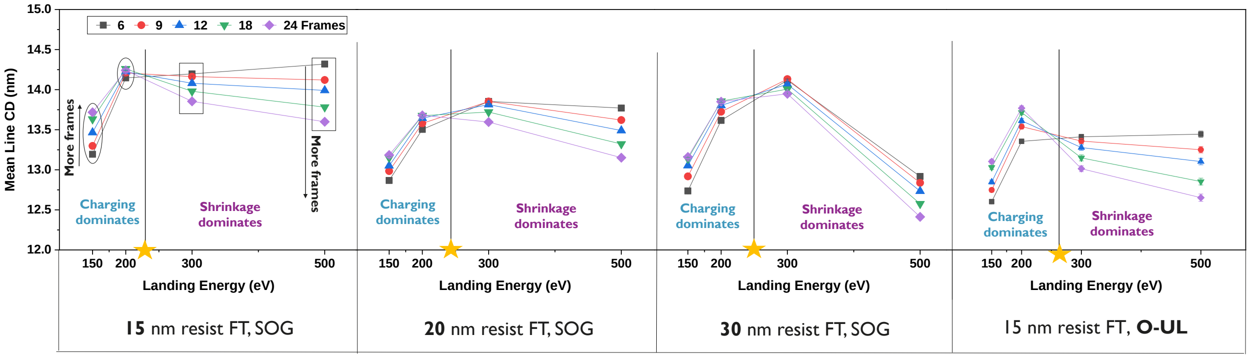

15 nm resist FT, SOG

20 nm resist FT, SOG

30 nm resist FT, SOG

15 nm resist FT, **O-UL**

Fig 8 Consistent trends between the mean CD and landing energies for the available wafer stacks.

3.2.1 CD shrinkage curves at the different landing energies

The photoresist feature width reduces upon the exposure to electron beam irradiation. The measurement starts with an unknown value of the virgin resist line, and upon the act of measurements with the e-beam, there are physical and chemical-induced interactions between the e-beams and the resist polymers that cause cleavage from some chemical groups and generation of volatile products. This leads to feature shrinkage, also known as resist slimming. The first measurement will be biased with this shrinkage which causes the uncertainty in the CDSEM measurement. By repeating the measurement at the same location (static repeat), the feature further shrinks, and shrinkage curves can be constructed. These curves mainly describe the reduction of the mean CD upon repeating the measurement at the same location (static repeats or runs) for probing the material-related shrinkage trends and measurement precision calculations for the different SEM conditions.

Figure 9 shows the shrinkage curves for the available resist thicknesses with the SOG and O-UL at the different landing energies and number of frames. The mean CD decreases upon repeating the measurements showing the shrinkage effects. At higher landing energy (300 eV and 500 eV), the whole curves shifts downwards when imaging with greater number of frames since the total dose increases. At low landing energies (150 eV and 200 eV), the curves shift upwards as the number of frames increases. As explained above, positive surface charging is evident at the low landing energy regime, which has its footprint in the shift of the whole shrinkage curves of the different number of frames.

From these curves, the mean CD difference between run 1 and run 2 for all the wafers and CDSEM conditions is calculated. For the SOG wafer, less difference in the mean CD between

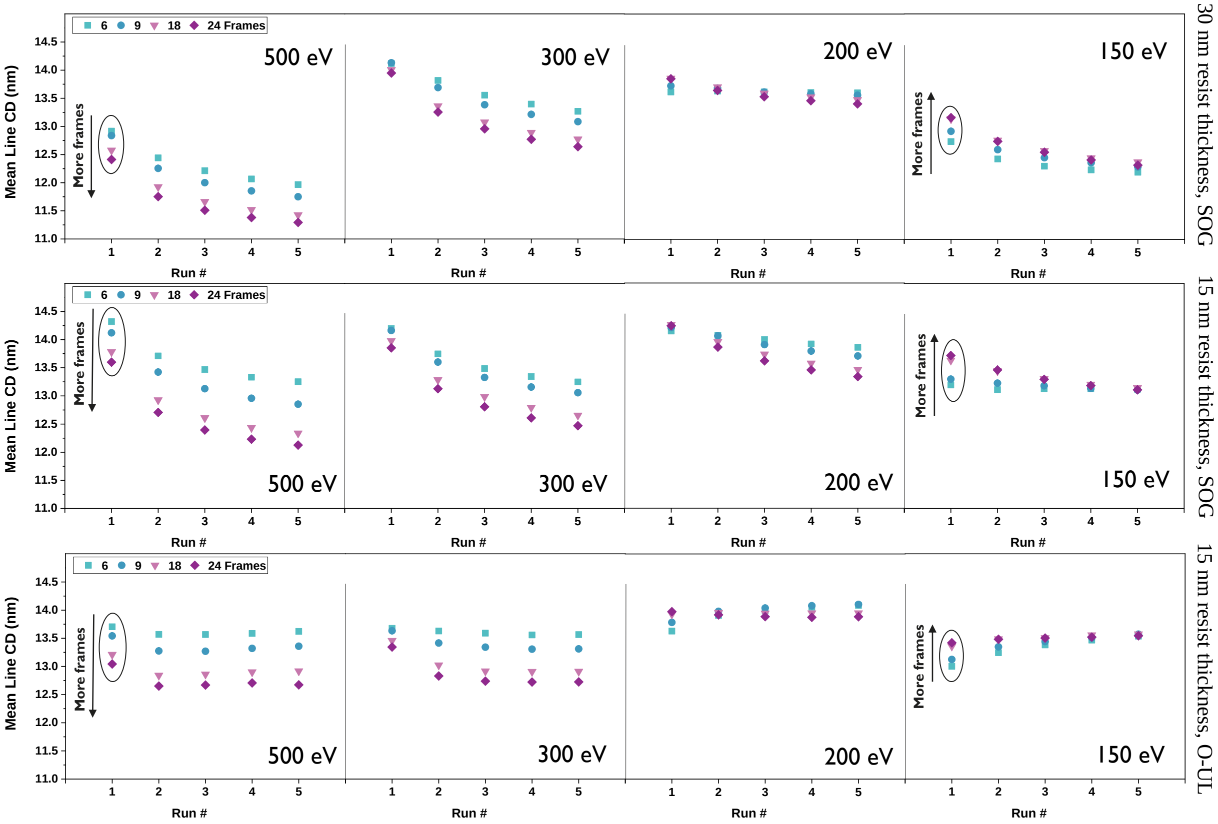

Fig 9 Shrinkage curves of the different landing energies and number of frames obtained for the available wafer stack.

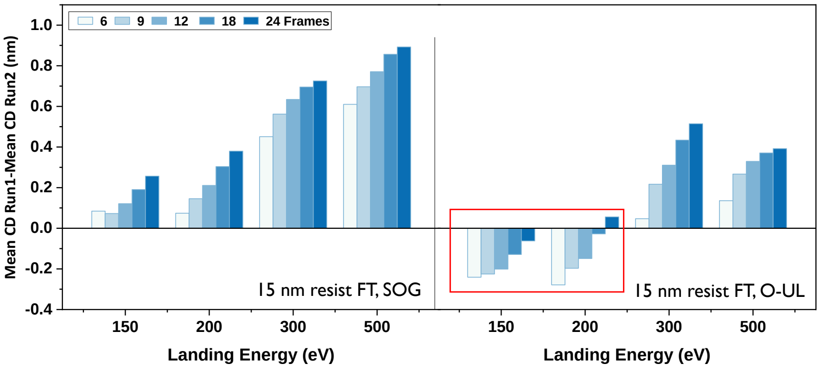

Fig 10 The mean CD difference between the first and second run for the 15 nm resist with the two available underlayers of SOG and O-UL.

run 1 and run 2 is observed at the lower landing energies and using lower number of frames, as shown in figure 10. This is one of the important merits of shifting towards lower landing energies as the beam effects on the resist features are reduced. Contrary to the SOG stack, the mean CD is observed to increase by repeating the measurements for the O-UL stack at lower landing energies of 150 eV and 200 eV. This further supports the possibility of surface charging of the O-UL space region that influences the resist line CD measurement. The SOG and O-UL have distinct chemical composition, therefore their charging response differs with the landing energies.

3.2.2 Mean CD Precision

Charging and shrinkage artifacts observed during measurements of the LVSEM are factors affecting the measurement precision, in addition to the smaller SNR observed for the thin resist. The carry-over corrected static CD precision has been calculated for all the SEM conditions of the landing energy and number of frames. For each SEM condition, 30 locations are measured, and for each location, five static repeats are performed without movement of the stage and a separate image is saved after each repeat. To calculate the image-based CD precision, firstly the mean CD for all the images from the 30 locations for each run is calculated. An average correction factor compensates for the shrinkage/charging artifacts for runs 2, 3, 4, 5, and it is calculated by subtracting the mean CD for each run (from the 30 available locations) from the mean CD of the first run (from the 30 available locations). Following the correction, the CD variance between the five runs is calculated for each measurement location. The CD precision value is 3 times the square root of the average variance between the five runs for all the 30 measurement locations. Figure 11 shows the image-based CD precision for the different SEM condition and resist thicknesses/underlayers. The precision values are acceptable for the low landing energies and thin resists.

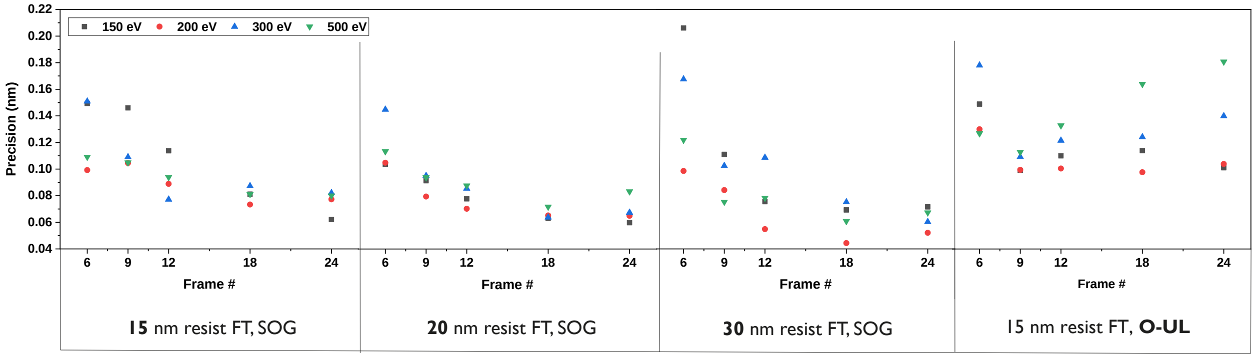

Fig 11 Mean CD carry-over corrected static precision per image calculated for the different landing energies and number of integration frames for the four available stacks under investigation.

3.3 *Roughness*

The line width roughness (LWR) measurements were reported to depend on the image pixel size, the CDSEM image noise, number of integration frames.[9] Within this study, the effect of the landing energy and number of integration frames on the measured unbiased LWR (uLWR) has been investigated. Figure 12 shows that the measured uLWR changes with the SEM measurement conditions of the landing energy and number of integration frames. The uLWR estimate appears to be affected by the landing energy and the number of frames of integration that modulates the image SNR. It is not determined if this effect is real or a metrology artifact.

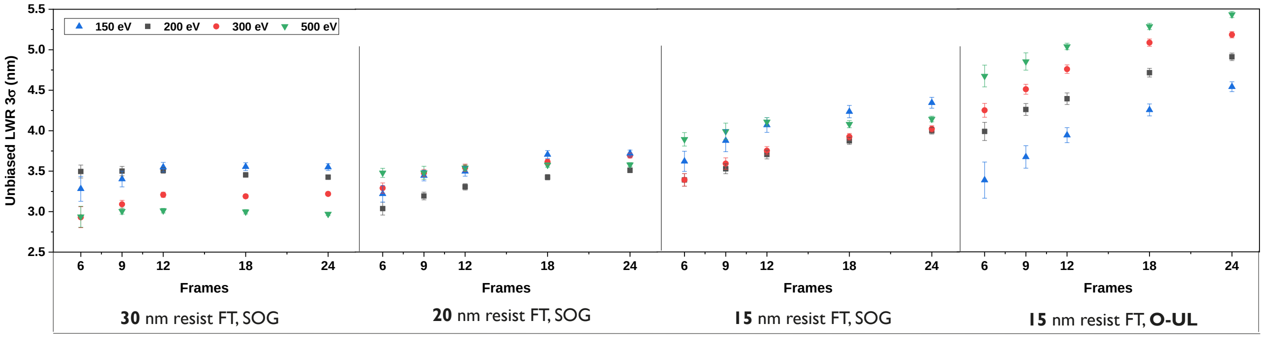

Fig 12 Unbiased LWR for the available available stack with the different measurement conditions of the number of frames and the landing energies.

4 Conclusions

The thin resist for high NA EUVL may pose metrology challenges because of the lower imaging contrast. This study investigated the use of ultra-low voltage aberration-corrected SEM for metrology of the thin resist. Because of the reduced impact of the e-beam on the resist feature and the small interaction volume, the image contrast between the resist and the underlayers is expected to be enhanced.

The dataset includes four stacks (variation between resist thicknesses and underlayer), four ultra-low landing energies, and five number of integration frames, repeated for five times. The goal is to investigate the benefits and issues of shifting towards ultra-low landing energy regime for the thin resist.

The analyses showed the thinner resists suffer from the smaller SNR, which is evident for all the measurement conditions at the different landing energies and number of frames. This represents the main challenge for the thin resist metrology. Charging of the resist and the underlayer showed its footprint in the mean CD estimate. By varying the landing energy and electron dose, two distinct regimes are observed, in which mean CD estimate is dominated either by charging at the low landing energy regime, or by shrinkage at higher landing energy regime. Additionally, comparing the SOG and O-UL, the O-UL stack has more charging artifacts observed in the mean CD shrinkage and linescan SNR metrics. This excessive charging can be considered as one of the criteria to exclude an underlayer type to another. For future experiments, we propose performing AFM measurements on the same SEM measurement location as a way to confirm the CD shrinkage magnitude for the different landing energies.

The optimal LE will depend on the materials stack in a non-trivial way because of the different secondary electron emission response of the resist and underlayers, which depends on their chemical nature and composition. The landing energy proved to be an important knob for metrology of the thin resist, allowing to achieve good measurement precision as well as enhancing the contrast for some resist/underlayers combination.

5 Acknowledgement

This work was executed as part of imec's core partner program. Joren Severi received funding from FWO (1SA8919N). This manuscript has been previously published in the SPIE conference Proceedings Volume 12053, Metrology, Inspection, and Process Control XXXVI; 120530P (2022) https://doi.org/10.1117/12.2613990.[11]

References

1 C. Zahlten, P. Gräupner, J. van Schoot, *et al.*, "High-NA EUV lithography: pushing the limits," in *35th European Mask and Lithography Conference (EMLC 2019)*, U. F. Behringer and J. Finders, Eds., **11177**, 43 – 51, International Society for Optics and Photonics, SPIE (2019).

2 G. F. Lorusso, C. Beral, J. Bogdanowicz, *et al.*, "Metrology of thin resist for high NA EUVL," in *Metrology, Inspection, and Process Control XXXVI*, J. C. Robinson and M. J. Sendelbach, Eds., **12053**, 120530O, International Society for Optics and Photonics, SPIE (2022).

3 S. Iida and T. Uchiyama, "Optimized structure of standard sample with programed defects for pattern inspection using electron beams," *Journal of Vacuum Science & Technology B* **36**(6), 06J502 (2018).

4 K. M. Monahan, J. P. H. Benschop, and T. A. Harris, "Charging effects in low-voltage SEM metrology," in *Integrated Circuit Metrology, Inspection, and Process Control V*, W. H. Arnold, Ed., **1464**, 2 – 9, International Society for Optics and Photonics, SPIE (1991).

5 M. T. Postek and A. E. Vladár, "Does Your SEM Really Tell the Truth?-How Would You Know? Part 4: Charging and its Mitigation," (October 21, 2015).

6 D. C. Joy and D. E. Newbury, "Low voltage scanning electron microscopy," *Microscopy and Microanalysis* **7**(S2), 762–763 (2001).

7 M. T. Postek, A. E. Vladár, and K. P. Purushotham, "Does your SEM really tell the truth? Part 2," (2014 May-Jun;36(3):347-55).

8 D. P. M Steigerwald, C Hendrich and K. Schubert, "A mirror-corrected scanning electron microscope," in *Proc. Frontiers of Characterization and Metrology for Nanoelectronics*, 51 – 55, International Society for Optics and Photonics (2013).

9 G. F. Lorusso, V. Rutigliani, F. V. Roey, *et al.*, "Unbiased roughness measurements: Subtracting out sem effects," *Microelectronic Engineering* **190**, 33–37 (2018).

10 C. A. Mack and B. D. Bunday, "Analytical linescan model for SEM metrology," in *Metrology, Inspection, and Process Control for Microlithography XXIX*, J. P. Cain and M. I. Sanchez, Eds., **9424**, 117 – 139, International Society for Optics and Photonics, SPIE (2015).

11 M. Zidan, D. Fischer, G. F. Lorusso, *et al.*, "Low-voltage aberration-corrected SEM metrology of thin resist for high-NA EUVL," in *Metrology, Inspection, and Process Control XXXVI*, J. C. Robinson and M. J. Sendelbach, Eds., **12053**, 120530P, International Society for Optics and Photonics, SPIE (2022).

List of Figures

1 (A) Interaction volume for high and low landing energy on thick and thin resist. (B) Effect of a charged underlayer on the emitted secondary electrons for thick and thin resist.

2 Schematic view of the mirror-corrected scanning electron microscope used in the study.[8]

3 SEM images for the 30 and 15 nm resist with the SOG and O-UL captured at different landing energies and 24 frames.

4 The effect of reducing the resist thickness on the linescan SNR at the different landing energies and number of frames of integration. Thinner resists always show reduced linescan SNR compared to thicker resists at the same measurement conditions.

5 The linescan SNR ratio dependence on the underlayer (O-UL & SOG) at the same resist thickness of 15 nm. Depending on the underlayers, different trends are observed between the SNR and the LE.

6 The linescan signal and grayscale image noise plotted separately for the different landing energies and number of frames for the two stacks of SOG and O-UL for the 15 nm resist. The landing energy clearly affects the linescan signal for the O-UL. The error bars on the data are contained in the size of the symbol.

List of Tables